Desalination and Water Treatment
www.deswater.com
doi: 10.1080/19443994.2015.1012333

57 (2016) 254–267
January

Taylor & Francis
Taylor & Francis Group

Synthesis and evaluation of methacrylic acid functionalized β-cyclodextrin based molecular imprinted polymer for 2,4-dichlorophenol in water samples

Hemavathy Surikumaran[a,b], Sharifah Mohamad[a,b,*], Norazilawati Muhamad Sarih[b]

[a]*Faculty of Science, Department of Chemistry, University of Malaya Centre for Ionic Liquids, Kuala Lumpur 50603, Malaysia, Tel. +603 79676751; Fax: +603 79674193; email: sharifahm@um.edu.my (S. Mohamad)*
[b]*Faculty of Science, Department of Chemistry, University of Malaya, Kuala Lumpur 50603, Malaysia*

Received 5 October 2014; Accepted 12 January 2015

ABSTRACT

Two imprinted polymers have been prepared through a simple radical polymerization technique in the presence of trimethylolpropane trimethacrylate as a cross-linker and 2,4-dichlorophenol (2,4-DCP) as the template molecule. For this purpose, imprinted polymers were synthesized using two different functional monomers: the first one using methacrylic acid (MAA) and the other one using methacrylic acid functionalized β-cyclodextrin (MAA-βCD). Structural characterization was carried out using various techniques for both polymers. The main objective of this paper is to report the synthesis and characterization of both imprinted polymers besides examining the application of MIP MAA-βCD polymer toward the recognition properties of 2,4-DCP. The results reveal that the highest removal for 2,4-DCP is obtained for the MIP MAA-βCD and suggests that the presence of β-CD plays a vital role in the binding capability of the polymer. The higher binding ability of MIP MAA-βCD to 2,4-DCP can be attributed to the presence of triple interactions including inclusion complex formation between β-CD and 2,4-DCP, whereas in MIP MAA only one interaction could possibly happen. MIP MAA-βCD has been applied to real water samples for the analysis of phenols.

Keywords: Molecular imprinted polymer; 2,4-dichlorophenol; β-cyclodextrin; Methacrylic acid; Removal; Water samples; Inclusion complex

1. Introduction

Water pollution is one of the major problems which have received serious attention of many researchers globally. Phenols are natural hazardous substances found in water resources. Phenol compounds, the priority pollutants controlled by the EPA have aroused researchers' serious concern because of their toxicity and possible accumulation in the environment [1] and recently, environmental aspects of substituted phenols have become increasingly important. Chlorophenols are harmful wastes mainly produced as by-products from the chemical processing of pesticides, herbicides, paint, paper production, and wood preservations [2], therefore, released continuously into the marine and

*Corresponding author.

Presented at the International Conference on Business, Economics, Energy and Environmental Sciences (ICBEEES) 2014, 19–21 September 2014, Kuala Lumpur, Malaysia

1944-3994/1944-3986 © 2015 Balaban Desalination Publications. All rights reserved.

freshwater environment, leading to the contamination of such ecosystems. The chlorination of natural waters also produces small amount of chlorinated phenols [3]. 2,4-dichlorophenol (2,4-DCP) are very common and have been highlighted by the US EPA in the Clean Water Act [4]. 2,4-DCP may cause carcinogenic and mutagenic effects to the living beings, since it can disturb the structure of cellular bilayer phospholipids [5]. They also create complicated problems to water bodies, such as unpleasant odor and taste in drinking water, the inhibition of the normal activities of microbial population in wastewater treatment plant, etc. Although there have been several legislations to control the pollutants release, significant concentrations of these kind of compounds and their metabolites are still found in the water system. In this context, adsorption technique serves as the efficient and economically feasible technology for the removal of various types of organic and inorganic pollutants [6–11] found in literature. The search for new material which is through a simple, sensitive, selective, and rapid method for the quantitative determination of pollutants in environmental samples seems to be an interesting research goal. A real and innovative analytical alternative is the use of the molecular imprinted polymer (MIP) as adsorbent. So far, we have noted the limited number of studies which have described the use of 2,4-DCP as the template for MIP synthesis in literature [12–14].

Molecular imprinting is a new technique of creating recognition sites for target analytes in synthetic polymers [15,16]. MIPs are tailor-made materials with high selectivity for a target compound which is known as template molecule [17]. Since their discovery in 1972, MIPs have gained considerable interest from scientists and engineers all over the world. Recently, smart polymers of this type have been used in many areas such as chromatography [18] or solid phase extraction (SPE) [19–21], sensors [22], organic synthesis [23], catalysis [24,25], drug discovery [26,27], combinatorial chemistry [28,29], drug delivery [30,31], etc. MIPs are effectively prepared by polymerization using a suitable monomer and cross-linker in the presence of template molecule. The functional groups of a template molecule (for which selectivity is expected) are involved in the formation of molecular interactions with the monomer(s) prior to a polymerization process [32]. The template molecules are removed after the polymerization. These empty imprinted sites are then accessible for the rebinding of the template which is complementary in shape, size, and positions of the functional groups to the template in a highly cross-linked polymer network [33]. The resulting imprinted polymers are robust, inexpensive and in many cases, possess an affinity and specificity that are suitable for industrial applications [34]. Considering the adaptability, high specificity and recognition that can be attained, the future of MIPs appears to be bright.

The essential key to the manufacture of the MIP with good binding properties is the optimization of the synthetic parameters. Commonly, in a non-covalent molecular imprinting system, the template molecule and monomer complexes are allowed to self-assemble first in a solution through non-covalent interactions such as hydrogen bonds, ionic bonds, hydrophobic interactions, van der Waals forces, etc. [35]. Hence, appropriate substituent of functional monomers is very important because their molecular interactions with the template are crucial for effective imprinting process [36]. The molecular imprinting provided by modified cyclodextrins (CD) which use a hydrophobic cavity that makes part of the binding site and gives strong interactions with the template molecule is very attractive, but yet has been little explored [32]. CD, described as supramolecular host, belong to a series of cyclic oligosaccharides. Specifically, β-cyclodextrin (β-CD) is formed by the binding of seven individual d-(+)-glucopyranose units through α-1,4-glycosidic oxygen bridges [37]. In this study, β-CD has been used since it can form inclusion complexes with variety of compounds by various kinds of intermolecular interactions due to the hydrophobic cavity [38]. Previous works [39–41] have shown interest in applying the inclusion process to chromatographic stationary phases and to sorbents that are able to collect organic pollutants and phenol compounds. Lately, the use of CD and modified CDs has received considerable attention in the molecular imprinting technique [42–45].

In this paper, we describe the synthesis of 2,4-DCP imprinted polymers obtained by a simple radical polymerization. A non-covalent approach was utilized to form MIPs using two different functional monomers and their respective non-imprinted polymers (NIP). Herein, we report on the characterization of these polymers using the Fourier transform infrared (FTIR), field emission scanning electron microscopy (FESEM), Brunauer–Emmett–Teller (BET), and X-ray diffraction (XRD) analysis. In addition, the thermal stability of these polymers was evaluated using thermo gravimetric analyses (TGA) and differential scanning calorimeter (DSC) analysis. The selective behavior of these imprinted materials toward 2,4-DCP in the presence of other phenol compounds has also been studied. Sorption experiments were conducted and the best imprinted polymer was selected on the basis of the optimal binding properties toward the template molecule and was successfully applied to real water samples.

2. Material and methods

2.1. Reagent and material

2,4-DCP, 2-chlorophenol (2-CP), 4-chloro-3-methylphenol (4-CMP), 2-nitrophenol (2-NP), and 4-nitrophenol (4-NP) were supplied by Sigma Aldrich (Steinheim, Germany). The functional monomer: methacrylic acid (MAA, ≥98%) is a commercial product from Sigma Aldrich, USA. β-CD was purchased from MP Biomedical, France. The cross-linkers: trimethylolpropane trimethacrylate (TRIM) and toluene-2,4-diisocyanate (TDI) were obtained from Sigma Aldrich, USA. Dimethylacetamide (DMAC), toluene, and methanol solvents were of the analytical reagent grade. The polymerization reaction initiator: benzoyl peroxide (BPO) was from Sigma Aldrich, USA. All other chemicals were of the highest quality available and used without further purification. For the preparation of aqueous solutions, ultrapure water (18 MΩ cm, Millipore Corporation, Rockland, MA, USA) was used.

Stock solutions were prepared by dissolving 1.0 g of 2,4-DCP and each of phenol compounds in 1.0 L methanol which was stored at 4˚C in the dark to prevent photodegradation. The standard solutions were prepared daily by diluting the appropriate volume of the stock solutions with water to obtain the desired concentrations.

2.2. Instruments

FTIR spectra were recorded using Perkin–Elmer RX1 FT-IR spectrometer (Perkin–Elmer Waltham, MA, USA). All the samples were run between 400 and 4,000 cm^{-1}. The technique used is known as attenuated total reflection mode [46]. The BET surface area and porous properties of polymers were determined from the nitrogen adsorption–desorption analysis at 77 K on the surface area analyzer (Quantachrome, Boynton Beach, FL, USA). The samples were previously degassed at 393 K, overnight. The FESEM images of imprinted and non-imprinted materials were performed on Quanta FEG 450 (FEI, Hillsboro, OR, USA) to analyze the morphology and surface structure of the adsorbents. UV–Vis spectrophotometer (Shimadzu, Japan) was used for the detection of 2,4-DCP at λ_{max} = 285 nm. ^{1}H NMR experiments were used to prove the interactions between the methacrylic acid functionalized β-CD (MAA-βCD) monomer and 2,4-DCP. ^{1}H NMR spectra were recorded on a LAMBDA JEOL 400 MHz FT-NMR spectrometer at room temperature. Tetramethylsilane (TMS) was used as an internal reference standard. The chemical shifts were reported in the ppm value relative to the TMS. For 2D NMR, the Nuclear Overhauser effect Spectroscopy (NOESY) spectrum was recorded in AVN 600 MHz (Bruker, Fallanden, Switzerland). Deuterated dimethylsulfoxide (DMSO-d_6) solvent which was used for NMR experiments was supplied by Merck (New York, USA). XRD patterns were taken using Cu–Kα irradiation with a Siemens D5000 X-ray diffractometer (Siemens, Frimley, UK) (voltage, 40 kV; current, 100 mA). Powder samples were mounted on a sample holder and then scanned from 5 to 30˚ at a speed of 3˚ min^{-1}. TA Instruments Q500 (Perkin Elmer, Waltham, MA, USA) was used to record TGA curves. The heating rate was set at 20˚C min^{-1} from 50 to 900˚C under nitrogen atmosphere. DSC (Perkin Elmer, Waltham, MA, USA) analysis was done by heating the samples from 30 to 400˚C at 20˚C min^{-1}. Phenol compounds were analyzed using an Agilent 7890A Gas Chromatography coupled with flame ionization detector (GC-FID) from Agilent Technologies Inc. (Santa Clara, CA, USA). GC column (Agilent HP-5MS column: 30 m × 0.32 mm i.d. and 0.25 μm film thickness) was used. The temperature program used was as follows: 35˚C held for 1 min, 35˚C min^{-1} to 220˚C, held for 8˚C min^{-1}. The injector and detector temperature was 250˚C and 300˚C, respectively. Helium was the carrier gas with a flow rate of 1.0 mL min^{-1} and nitrogen was used as the make-up gas with a flow rate of 32.4 mL min^{-1}. One micro liter of sample was injected manually into the injection port under split less mode.

2.3. Synthesis of MAA-βCD monomer

The stoichiometric ratio in this case was 0.5 M MAA: 1 M TDI: 0.5 M β-CD. This ratio is based on the previous study reported by Sreenivasan [47] with slight modification. The chosen molar concentration was to react with only one –OH group of β-CD. Firstly, the MAA and TDI were allowed to mix in 40 mL DMAC; then 0.1% dibutyltin dilaurate (catalyst) was added and the solution was stirred magnetically for 1 h at room temperature under nitrogen gas. At this stage, a few drops of this solution were subjected to the FTIR analysis. Finally, a calculated amount of β-CD was added to this solution mixture together with 10 mL DMAC and further stirred for about 2 h. The final product, MAA-βCD monomer was characterized using the FTIR. The commercially available monomer MAA also was subjected to FTIR analysis. The synthesis route for the preparation of functional monomer, MAA-βCD is shown in Fig. 1.

2.4. Preparation of the 2,4-DCP imprinted polymers

The imprinted polymers (MIP MAA and MIP MAA-βCD) were prepared using the bulk polymerization

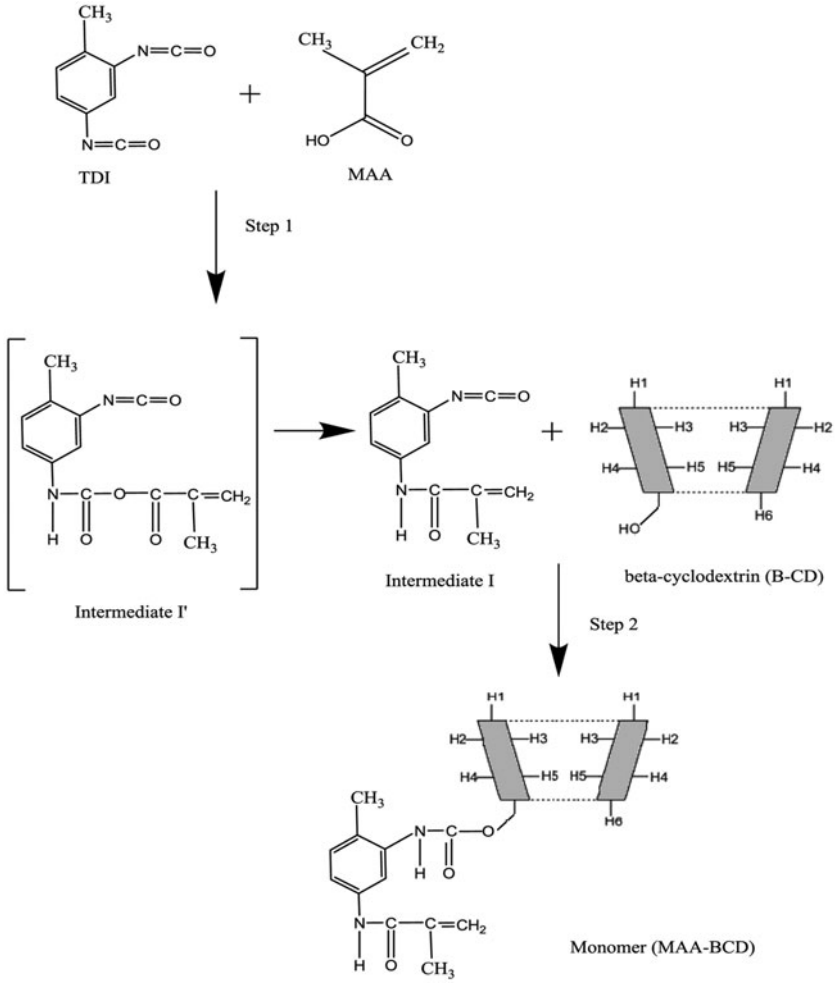

Fig. 1. The synthesis route for the MAA-βCD monomer.

method. In this study, we have chosen the molar ratio of the template molecule and functional monomer to cross-linker (1:4:20) as used in the traditional preparation method [48]. For the synthesis of MIP MAA, the template molecule (2,4-DCP), functional monomer (MAA) and the cross-linker (TRIM) were dissolved in toluene. Next, the organic solvent soluble initiator (benzoyl peroxide, 1 g) was added. The homogeneous solutions were purged with nitrogen gas for 10 min and then the flask was sealed. Subsequently, the thermal polymerization was carried out in a water bath at 70°C for 24 h under a nitrogen atmosphere. The obtained polymers were ground and sieved in order to get regular-sized particles. Meanwhile, for the preparation of MIP MAA-βCD, the same procedure as above was followed but MAA-βCD and DMAC were used as the monomer and porogen, respectively. The template was removed by washing the polymers with methanol/acetic acid (3:1 v/v) solution thrice. Then, the polymers were extensively washed with water. The washing procedure was repeated until the 2,4-DCP molecule could not be detected by the UV–Vis spectrophotometer at $\lambda_{max} = 285$ nm. NIPs (NIP MAA and NIP MAA-βCD) were prepared and treated in a similar manner, but without the addition of 2,4-DCP molecule.

2.5. Sorption experiments

The binding experiments were performed to evaluate the binding ability of both the MIP and NIP polymers. Non-competitive binding experiments were carried out to determine their selectivity and assess the intermolecular interactions in the polymer matrix. All experiments were performed in triplicates. To evaluate the selectivity of the MIP MAA-βCD for 2,4-DCP, competitive adsorption experiments were carried out in aqueous solution containing 2,4-DCP and series of structural analogs such as 2-CP, 4-CMP, 4-CP, 2-NP, and 4-NP. About 20 mg of MIPs or NIPs were mixed with 10 mL solution containing 10 mg L^{-1}

of each phenol in a vial that was shaken at 298 K for 2 h. GC-FID was used to measure the residual concentration of the five analytes in each supernatant solution, respectively. The distribution coefficient, K_d can be evaluated using Eq. (1):

$$K_d = \frac{[C_i - C_f] \times v}{M} \quad (1)$$

where C_i and C_f is the initial and final concentration. v (L) is the volume used and M (g) is the weight of MIP MAA-βCD. The selectivity coefficient, k for the binding of 2,4-DCP in the presence of interferences can be evaluated by Eq. (2):

$$k = \frac{K_d\ (2,4-\mathrm{DCP})}{K_d\ (\mathrm{phenolic})} \quad (2)$$

where phenolic represents the 4-CMP, 2-CP, 4-NP, and 2-NP. The effect of imprinting on selectivity is evaluated by comparing k values of the imprinted polymers with other studied phenols. k', a relative selectivity coefficient can be defined as Eq. (3):

$$k' = \frac{k\ \text{imprinted}}{k\ \text{non-imprinted}} \quad (3)$$

2.6. SPE of real water sample

Thirty milligram of MIP MAA-βCD was packed manually into an empty 3 mL SPE polypropylene cartridge with frits placed on top and bottom to avoid adsorbent loss. Firstly, the SPE cartridges were conditioned by passing 5 mL of methanol and 5 mL of water. Then, 15 mL of spiked tap water or river water (1 microgram L^{-1} of phenol mixture) adjusted to pH 7 was passed through the cartridge at a flow rate of 0.5 mL min^{-1}. The cartridge was dried for 30 min by passing air after the sample loading. The retained phenols were eluted from the MIP MAA-βCD sorbent using 2 mL of methanol containing 1% of acetic acid. Finally, the eluates were analyzed using GC-FID. The river water was collected daily from Taman Jaya, Petaling Jaya, Kuala Lumpur meanwhile the tap water samples were taken directly from the tap in a laboratory at University of Malaya.

2.7. Preparation of inclusion complex (MAA-βCD-DCP)

The inclusion complex of MAA-βCD with 2,4-DCP was prepared using the conventional kneading method [49]. Equimolar amounts of MAA-βCD and 2,4-DCP were knead with mortar and pestle in minimal ethanol to form a homogeneous paste. The complex was grind for approximately 30 min and dried to constant mass. After drying, the obtained white powder (MAA-βCD-DCP inclusion complex) was subjected to the ^{1}H and 2D NMR analysis.

3. Results and discussion

3.1. Preparation of MAA-βCD monomer

Our experimental results show that the reactions between TDI and MAA are stoichiometric, direct addition reactions as shown in Fig. 1. It is well known that isocyanate group can easily react with compounds containing active proton including alcohol and acid in stoichiometric quantities [50]. From Fig. 1, it can be seen that intermediate I′ containing an anhydride and a carbamate group was formed at the consumption of carboxyl group in MAA. Intermediate I is unstable and it converts to methacrylic amide containing an isocyanate group. Intermediate I contains methacrylic amide and N=C=O indicating that only one of the two N=C=O groups in TDI took part in the reaction. The unreacted N=C=O in Intermediate I can be used for further isocyanation with βCD to yield MAA-βCD. When the TDI introduced, one of the isocyanate group would randomly react with the hydroxyl groups of the MAA and the other one would react with β-CD molecules subsequently to form urethane linkages [51]. β-CD molecule was chosen as polymer building units based on its unique capability to form inclusion complex with the template molecule. This monomer later on will be used in the molecular imprinting technique to produce MIP MAA-βCD and its counterpart NIP (NIP MAA-βCD). Structural analysis further confirmed that the monomer was successfully prepared using this two-step isocyanation process.

3.2. Characterization of MIP MAA and MIP MAA-βCD

3.2.1. Fourier transform infrared analysis

FTIR was utilized to assess the presence of the functional groups on the adsorbent surface in the range of 400–4,000 cm^{-1}. The FTIR spectra of MIP MAA-βCD, MIP MAA, and their respective monomers (MAA and MAA-βCD) are shown in Fig. 2. In Fig. 2(a), the broad peak was observed at 2,930 cm^{-1} due to the C–H stretching vibrations in MAA. While in the spectrum of MAA-TDI, (Fig. 2(b)) the obvious peaks were observed at 3,304 and 2,283 cm^{-1} which corresponds to carbamate group (–NHCO) and

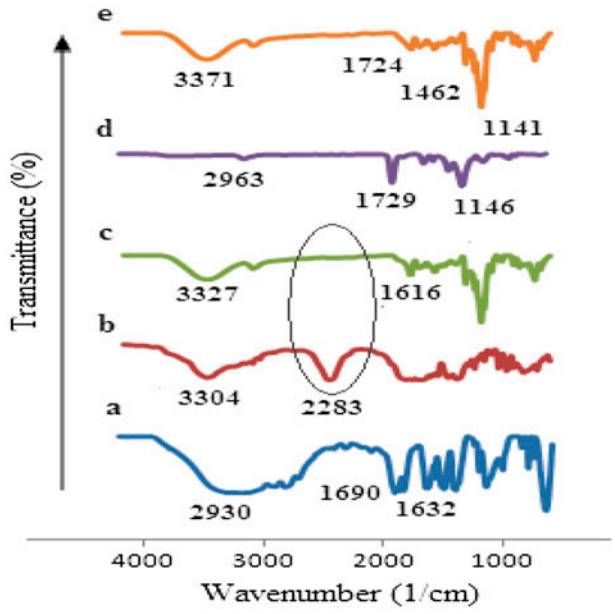

Fig. 2. FTIR spectra of (a) MAA, (b) MAA-TDI, (c) MAA-βCD, (d) MIP MAA, and (e) MIP MAA-βCD.

N=C=O (isocyanate peak of TDI). The spectrum of MAA-βCD (Fig. 2(c)) shows the complete disappearance of N=C=O peak at 2,283 cm^{-1} and the formation of a new carbamate group at 3,327 cm^{-1} after reacting with β-CD. The absence of the N=C=O group shows that the reaction with −OH group of β-CD is completed. The presence of C=C from MAA at 1,616 cm^{-1} indicates that the double bond of the MAA is intact in the monomer. This is very important because this double bond will be used later in the cross-linking process with TRIM. Therefore, this result has been evidence for the formation of MAA-βCD monomer which was formed between MAA-TDI and β-CD. Strong peaks around 2,963, 1,729, 1,146 cm^{-1} and 3,371, 2,953, 1,724, 1,462, 1,257 and 1,141 cm^{-1} were observed in the spectrum of MIP MAA (Fig. 2(d)) and MIP MAA-βCD (Fig. 2(e)), respectively. The peak at 3,371 cm^{-1} in MIP MAA-βCD was due to the formation of the –NHCO group between –OH (β-CD) and N=C=O (MAA-βCD monomer). In both MIPs, the band at 2,963 and 2,953 cm^{-1} was observed due to the symmetric and asymmetric C–H stretching vibrations. The obvious absorption band (C=O) of the TRIM located at 1,729 and 1,724 cm^{-1} in both MIPs indicates that the cross-linking reaction was successful. Whereas, a band centered at 1,141 and 1,146 cm^{-1} was due to the C–O stretching of 2,4-DCP. The bands around 1,462 cm^{-1} were suggested to be the aromatic ring stretching vibrations of 2,4-DCP and the band at 1,257 cm^{-1} was assigned to the stretching vibration of the C–OH of alcoholic groups and carboxylic acids from MAA-βCD. All the significant peaks of β-CD and MAA also appeared in the spectrum of MIP MAA-βCD. Thus, it could be inferred that the structural characteristics of β-CD and MAA were well maintained in the MIP MAA-βCD. Surprisingly, new absorption bands were not observed in the spectrum of MIP MAA-βCD when 2,4-DCP was loaded onto the imprinted polymer. Only the wave numbers of some absorption bands shifted to high or short absorption wave numbers. This is an indication for the formation of the inclusion complex between 2,4-DCP and β-CD in MIP MAA-βCD during the imprinting process [52].

3.2.2. Morphological study

Imprinted polymers are generally insoluble materials whose subsequent use depends on their morphology in terms of the particle's shape, size, and the porous texture of the material. Therefore, it is important to determine the morphology of the imprinted polymers as it can affect their subsequent molecular recognition properties and/or their modes of application [46]. The FESEM was employed to analyze the surface of the imprinted particles prepared from the MAA monomer: MIP MAA/NIP MAA and β-CD modified MAA monomers: MIP MAA-βCD/NIP MAA-βCD. The obtained micrographs are presented in Fig. 3. Generally, the micrographs show some dissimilarity between the MIPs and NIPs, prepared from different monomers. The polymerization with MAA led to the morphology like a conglomerate of beads as shown in Fig. 3(a). The surface of the imprinted polymers prepared using MAA is rougher and denser with large pores as shown in Figs. 3(a) and (b). MIP MAA polymers possess small cavities between larger ones with a diameter less than 2 μm which are joined together into the conglomerates when the cross-linker TRIM was used. Referring to Fig. 3(c), the shape difference of MIP MAA-βCD from MIP MAA particles could be resulting from the presence of β-CD cavities and the effect of the porogen during the polymerization process. The porogen plays an important role in the final polymer morphology, influencing its surface morphology and the pore diameter [53]. DMAC solvent was used to prepare the MIP MAA-βCD because MAA-βCD monomer was insoluble in toluene and the polymer mixture was not homogeneous. MIP MAA synthesized using non-polar solvent (toluene) produces bigger conglomerates and particles with a beaded appearance. Meanwhile, MIP MAA-βCD particles synthesized using polar aprotic solvent (DMAC) possesses a loose and more porous structure with

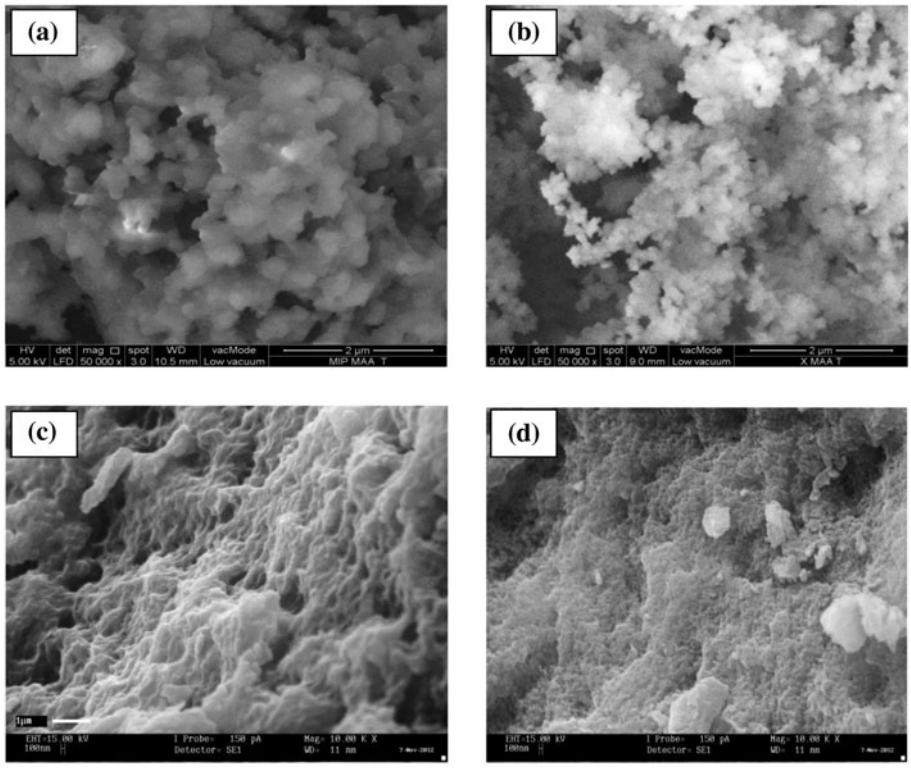

Fig. 3. SEM micrographs of the imprinted particles prepared from monomer MAA (a) MIP MAA, (b) NIP MAA and monomer MAA-βCD, (c) MIP MAA-βCD, and (d) NIP MAA-βCD using cross-linker, TRIM.

many small cavities responsible for the high capacity of this polymer. This finding is supported by the BET result which suggests the presence of micropores in MIP MAA-βCD. Generally, the surface of the NIPs formed as irregular particles seems to be smoother, compact, and less porous compared to their counterparts. This continuously smooth morphology explains the low capacity of NIPs to 2,4-DCP. As a conclusion, the presence of the β-CD cavities in the MIP MAA-βCD polymer network is responsible for imprinting cavities that are favorable for the rebinding of template molecule.

3.2.3. Brunauer–Emmett–Teller analysis

Nitrogen adsorption–desorption analysis was used to evaluate the BET surface area, total pore volume and pore size of the polymers. The corresponding isotherms are presented in Fig. S1. The specific surface areas of MIPs were higher than their corresponding NIPs (see Table 1). The N_2 adsorption–desorption isotherms of MIP MAA and NIP MAA (inset diagram) exhibited a resolved type IV isotherm with a steep desorption branch and a H3 type hysteresis loops, indicating the existence of many mesopores in the polymer. Meanwhile, the isotherm profiles for both MIP MAA-βCD and NIP MAA-βCD were a mixture of types I and IV, suggesting that they had a mixed microporous and mesoporous structure. The specific surface area, total pore volume, and average pore size of MIP MAA-βCD were 2.441 $m^2 g^{-1}$, 0.022 $cm^3 g^{-1}$, 1.587 nm, while these parameters were obviously different from those of MIP MAA (121.373 $m^2 g^{-1}$, 0.247 $cm^3 g^{-1}$, and 8.056 nm). According to the IUPAC definition, MIP MAA-βCD and NIP MAA-βCD mainly possess micropores (pore size < 2 nm) [54], while MIP MAA and NIP MAA possess mesopores (2 nm < pore size < 50 nm). It might seem confusing that the MIP MAA-βCD had many imprinted cavities and should have larger surface area and pore volume than MIP MAA. But, we found that MIP MAA-βCD had a low surface area compared to that of the MIP MAA in dry state. However, this polymer had a hydrogel like nature with a high swelling capacity in water and with many cavities; consequently, its networks could sufficiently expand to allow a rapid diffusion process for the analyte of interest. Therefore, the polymer pore size and surface area could greatly increase after swelling. A similar phenomenon has been observed by Li and his co-workers [14].

Table 1
Results of the BET analysis for the four polymers studied

Polymers	Specific surface area ($m^2\ g^{-1}$)	Total pore volume ($cm^3\ g^{-1}$)	Average pore size (nm)
MIP MAA	121.373	0.247	8.056
NIP MAA	74.650	0.158	7.655
MIP MAA-βCD	2.441	0.022	1.587
NIP MAA-βCD	2.225	0.019	1.465

3.2.4. X-ray Diffraction analysis

XRD analysis provides further evidence for the formation of MIP MAA-βCD as demonstrated in Fig. 4. Fig. 4 shows the XRD patterns of MIP MAA and MIP MAA-βCD. Many sharp peaks are clearly visible in the diffractogram of MIP MAA-βCD at 9.7˚, 11.6˚, 12.6˚, 13.1˚, 17.3˚, and 21˚ which belongs to β-CD molecule [55]. While in the diffractogram of MIP MAA, no clear peaks are visible. The broad asymmetric peak at around $2\theta = 15^\circ$ suggests that the degree of crystallinity decreased compared to the MIP MAA-βCD. Hence, from this result we can conclude that the MIP MAA-βCD exhibited some crystallinity due to the presence of β-CD molecule, whereas MIP MAA was an amorphous polymer.

3.2.5. Thermal analysis

In this work, the comparison between the thermal stability of MIP MAA-βCD and MIP MAA was evaluated using TGA and DSC. The results are presented in Fig. 5(a) and (b), respectively. As can be seen from Fig. 5(a), MIP MAA-βCD starts to decompose at 340˚C and MIP MAA decomposes at 290˚C. Whereas, it can be observed in Fig. 5(b), that the MIP MAA displays completely different trends than the MIP MAA-βCD. There are three stages involved in the DSC analysis of

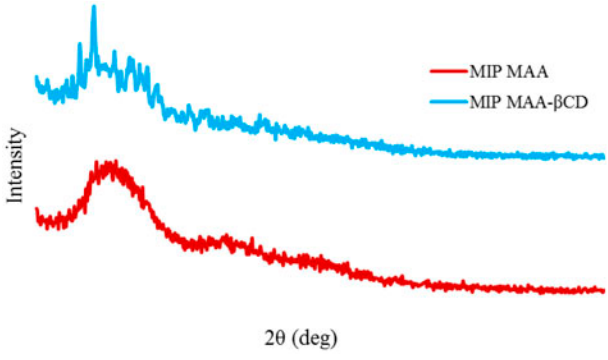

Fig. 4. X-ray diffractogram of MIP MAA-βCD and MIP MAA.

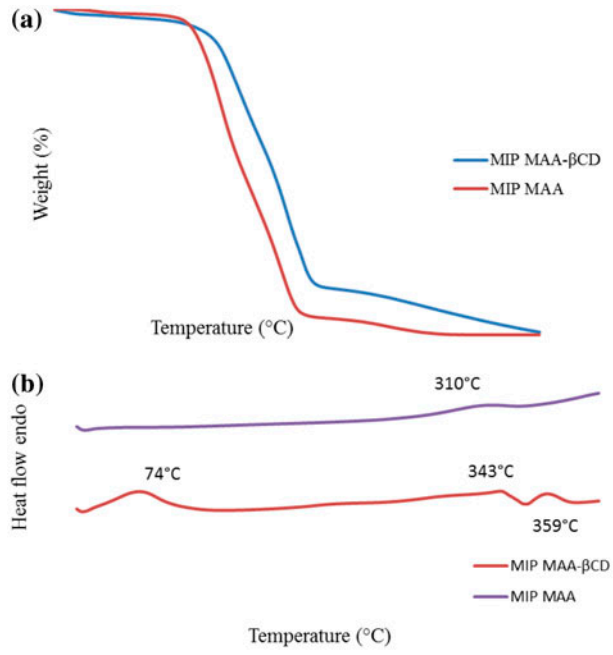

Fig. 5. (a) TGA curves and (b) DSC curves of MIP MAA-βCD and MIP MAA.

MIP MAA-βCD, while only one stage involved in MIP MAA. Two strong endothermic peaks were observed for MIP MAA-βCD at 74 and 359˚C which was associated with loss of water molecules from β-CD cavity and the latter due to the polymer decomposition. An exothermic peak at 343˚C which was corresponding to curing of the polymer, confirmed that there is a high degree of cross-linking in the MIP MAA-βCD [56]. Meanwhile for MIP MAA, the only peak appeared at 310˚C which was lower than MIP MAA-βCD. Both TGA and DSC results suggest that the MIP MAA is thermally less stable than MIP MAA-βCD. This can be explained by the fact that the presence of β-CD molecule increases the thermal stability of MIP MAA-βCD.

3.3. Sorption studies of 2,4-DCP

The imprinted polymers synthesized using β-CD modified monomer; MIP MAA-βCD and NIP

MAA-βCD were applied to sorption studies to compare their performance with polymers prepared using unmodified monomer, namely, MIP MAA and NIP MAA. The molecular imprinting factor (IF) for the evaluation of the recognition selectivity was calculated using the equation $IF = K_{MIP}/K_{NIP}$, where K_{MIP} was the capacity factor of the 2,4-DCP on the MIP and K_{NIP} was that on the NIP [57]. Table 2 gives the imprinting factor, IF values for the 2,4-DCP in two different MIPs and the corresponding NIPs. The binding capacity of 2,4-DCP was better in the MIPs than in the NIPs. This result confirms the imprinting effect. In addition, MIP MAA-βCD was shown to be superior to MIP MAA in terms of imprinting factor. Generally, most MIP systems are based on MAA monomers alone, because its carboxyl group is the most common hydrogen bonding and acidic functional group in molecular imprinting [58]. However, our finding reveals that the functionalization of the MAA using β-CD had contributed to a much better imprinting effect toward 2,4-DCP than the unmodified MAA. The difference in the binding capacity mainly attributed to the presence of β-CD cavities in the MIP MAA-βCD polymer network which enhances the molecular recognition process. Moreover, MIP MAA-βCD had higher binding capacity to its template (2,4-DCP) compared to NIP MAA-βCD. The binding capability of NIP MAA-βCD toward 2,4-DCP was lower compared to MIP MAA-βCD probably due to the non-specific interaction and absence of imprinted sites. In conclusion, MIP MAA-βCD was the most suitable sorbent for 2,4-DCP.

3.4. Selectivity of MIP MAA-βCD toward 2,4-DCP

Previous result suggests that MIP MAA-βCD had the highest imprinting effect among all the polymers studied. The binding selectivity of this imprinted material toward 2,4-DCP in the presence of other phenols was further evaluated and presented in Table S1. Selectivity studies were performed on MIP MAA-βCD for the structurally related molecules in dynamic binding experiments as described in the previous section. MIP MAA-βCD exhibited higher molecular recognition selectivity for 2,4-DCP. The selectivity data confirmed that the selectivity of the MIP MAA-βCD for 2,4-DCP was significantly superior than the NIP MAA-βCD. This finding can be explained by the fact that generally MIPs can recognize their template molecules via the existence of memory cavities with fixed size, shape, binding sites, and specific binding interaction between the target molecule and sites [59]. In addition, the NIP adsorbed template less than that of MIP since NIP had not generated specific recognition sites due to the absence of template molecule. Therefore, only the non-specific adsorption was present in the case of NIP [60]. The presence of β-CD cavities in MIP MAA-βCD basically enhanced the selectivity toward the template molecule. It is well known that β-CD can form inclusion complex with phenols [61,62], so in this current work inclusion complex formation could be formed as the cavity of β-CD was maintained in the polymer network.

3.5. Application to real water sample

The developed SPE method using MIP MAA-βCD as a sorbent was applied to the real water samples such as river and tap water to analyze phenols. None of the target phenols were detected in these water samples under the studied conditions. About 15 mL of river and tap water samples adjusted to pH 7 and then spiked with phenol mixtures at 1.0 microgram L^{-1} levels to assess recovery. High recoveries were obtained for both tap and river water samples in the range of 98–115% with the relative standard deviation (RSD) values of 2–4% (the result is shown in Table S2). These satisfactory results show the suitability of MIP MAA-βCD as SPE sorbent for the analysis of phenols in aqueous samples.

3.6. Interaction between MAA-βCD and 2,4-DCP

3.6.1. ^1H NMR Spectra

The preservation of the pre-polymerized host/guest structure in a polymer matrix explains the principle of molecular imprinting. Consequently, it is vital that the template and the monomer can form stable complexes via hydrogen bonding, ionic bonding, or

Table 2
Comparison of the imprinting factor, IF values of 2,4-DCP with respect to four studied polymers

Analyte	Capacity factor (K_{MIP})		Capacity factor (K_{NIP})		Imprinting factor (K_{MIP}/K_{NIP})	
	MIP MAA-βCD	MIP MAA	NIP MAA-βCD	NIP MAA	MIP MAA-βCD	MIP MAA
2,4-DCP	5.19	4.73	2.76	3.34	1.88	1.42

other interaction forces in the pre-polymerization mixture [58]. The interaction between template, 2,4-DCP and monomer, MAA-βCD was studied to understand the molecular recognition mechanism.

^{1}H NMR spectra is a useful technique to confirm the formation of an inclusion complex and can provide useful information on the inclusion mechanism of CDs with the guest molecules. Changes of chemical shift of particular nuclei in the host molecule can verify the formation of inclusion complex in solution, since critical changes in the microenvironment are known to happen in the CD inclusion complex [49]. The ^{1}H NMR spectrum of MAA-βCD, 2,4-DCP, and inclusion complex (MAA-βCD-DCP) recorded in DMSO-d_6 solvent are shown in Fig. S2. A comparison of ^{1}H NMR chemical shifts for 2,4-DCP, MAA-βCD, and their inclusion complex was shown in Table 3. The OH_D proton of 2,4-DCP obviously shifted upfield from 9.83 to 9.063 ppm in the presence of MAA-βCD. H_C protons of 2,4-DCP are at downfield because it is surrounded by two chlorine atoms (electron withdrawing atom) that make the H_C atom more de-shielded. To explore further into the inclusion complex formation, we are interested in the protons inside the β-CD cavity, H_3, and H_5, also H_6 proton which is located at the cavity rim at the narrow end of the molecule. As expected, the most obvious chemical shifts occur at H_3 and H_5 protons of β-CD molecule. On the other hand, the chemical shifts of H_1, H_2, H_4, and H_6 which are located on the outer surface of β-CD are only slightly affected by the 2,4-DCP molecule. In the case of inclusion complex (MAA-βCD-DCP), the change in the chemical shift (δ ppm) for H_3 is 0.0592 while for H_5 is 0.0617. Since H_3 and H_5 have larger δ ppm values, we conclude that 2,4-DCP had been penetrated into the hydrophobic cavity of β-CD molecule. All these results have revealed the formation of inclusion complex between 2,4-DCP and MAA-βCD.

3.6.2. 2D NMR Spectra

2D NMR is a powerful tool for investigating intermolecular interaction and to gain more information on the conformity of the inclusion complex [63]. To obtain further information on the inclusion complex formation, the 2D NOESY technique was employed. NOESY is one of the most useful techniques as it allows correlating nuclei through space (distance smaller than 5Å). The cross peaks in the spectra was originated from the interaction between the protons of

Table 3
^{1}H NMR chemical shift (ppm) for MAA-βCD, 2,4-DCP, and inclusion complex (MAA-βCD-DCP)

	MAA-βCD (δ ppm)	DCP (δ ppm)	MAA-βCD-DCP (δ ppm)	Δ MAA-βCD-DCP (δ ppm)
MAA				
H_a	1.9445		1.9408	−0.0037
H_b	2.7713		2.7676	−0.0037
TDI				
H_c	7.7248		7.7481	0.0233
H_d	7.9205		7.9079	−0.0126
H_e	8.2204		8.2088	−0.0116
H_f	2.9306		2.9245	−0.0061
H_g	8.4229		8.4547	0.0318
β-CD				
H_1	4.8203		4.8179	−0.0024
H_2	3.3272		3.3156	−0.0116
H_3	3.6213		3.5621	**−0.0592**
H_4	3.3620		3.3406	−0.0214
H_5	3.6012		3.5395	**−0.0617**
H_6	3.6482		3.6231	**−0.0251**
OH_2	5.5806		5.7265	0.1459
OH_3	5.6752		5.6795	0.0043
OH_6	4.4487		4.4707	0.0220
DCP				
H_A		6.9499	6.9377	−0.0122
H_B		7.1879	7.1952	0.0073
H_C		7.3697	7.4216	0.0519
OH_D		9.8300	9.0630	**−0.7670**

Note: The bold values indicate high chemical shifts obtained for protons in the inclusion complex.

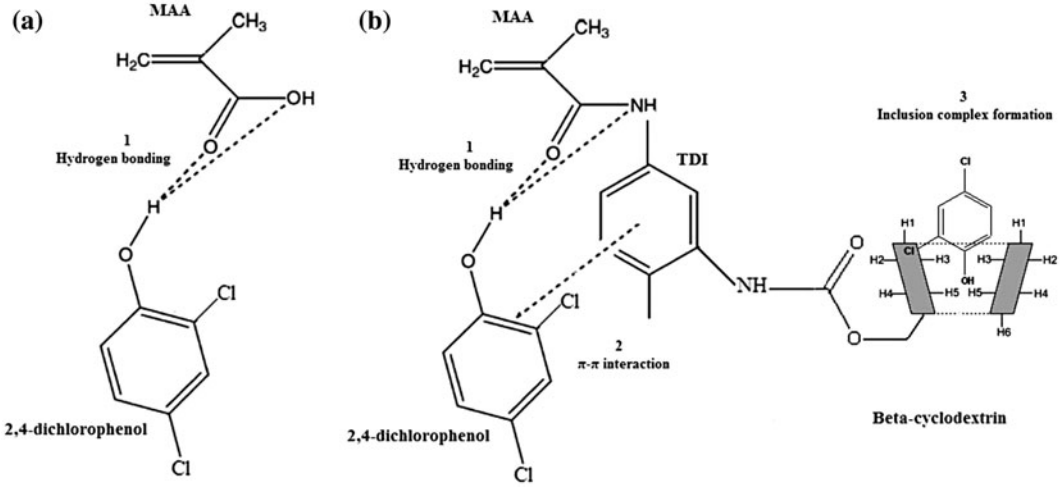

Fig. 6. The proposed interaction mechanism between functional monomer (a) MAA and (b) MAA-βCD with 2,4-dichlorophenol (template).

2,4-DCP and MAA-βCD (shown in Fig. S3). The cross peaks of β-CD (3.5–3.6 ppm, H_3, and H_5), MAA (1.9–2.7 ppm, H_a, and H_b), TDI (7.7–8.4 ppm), and 2,4-DCP (6.9–9.1 ppm, H_A, H_B, H_C, and OH_D) demonstrate strong intensity. The strong correlation suggests that the protons of 2,4-DCP are strongly interacting with β-CD cavity. Hence, from the NOESY spectra we can further confirm that the 2,4-DCP molecules have entered the cavity of the β-CD in MAA-βCD monomer via the inclusion complex formation.

3.7. Recognition mechanism of 2,4-DCP onto MIP MAA-βCD

There are various types of possible interactions which correspond to the recognition ability of MIP MAA-βCD toward 2,4-DCP as shown in Fig. 6. NOESY spectra suggest that there is a strong interaction between the MAA-βCD monomer and 2,4-DCP. 1) The formation of hydrogen bonding between hydrogen atom of 2,4-DCP and nitrogen or oxygen atom in MAA-βCD monomer. 2) π–π interaction between the aromatic ring of 2,4-DCP and benzene ring of TDI in the MAA-βCD monomer. 3) The inclusion complex formation between β-CD cavity in MAA-βCD and 2,4-DCP molecules. As described in Section 3.6, ^{1}H and 2D NMR results have confirmed the formation of inclusion complex in aqueous media. Because of the hydrophobic nature of the template and the hydrophobic center of the β-CD cavity, the template had been inserted into the cavity of the β-CD in the rebinding process in aqueous media. In contrast to MAA-βCD, only one interaction (hydrogen bonding) is possible in the MAA (see Fig. 6(a)). A similar phenomenon was observed by Ersoz et al. who have reported on the imprinting of nitrophenol using MAA monomer [64]. In conclusion, the presence of triple interactions as stated above between MAA-βCD and 2,4-DCP is responsible for the high recognition ability of the MIP MAA-βCD for 2,4-DCP in water samples which was resulted from the modification of MAA monomer using β-CD.

4. Conclusions

Two imprinted polymers were successfully prepared, characterized, and their removal efficiency for 2,4-DCP in water samples was compared. The highest removal efficiency for 2,4-DCP was achieved with MIP MAA-βCD which was prepared using MAA-βCD monomer and cross-linker, TRIM in DMAC solvent. The SEM and BET results show that MIP MAA-βCD polymer exhibited porous structure which had resulted in the highest removal efficiency which is useful from an analytical point of view. TGA and DSC results show that the presence of βCD molecule is responsible for high thermal stability of MIP MAA-βCD. The comparison of the binding abilities of 2,4-DCP and its structural analog to MIP MAA-βCD shows that strong interactions between the template molecule and β-CD cavity in the functional monomer govern the recognition mechanism through the inclusion complex formation. MIP MAA-βCD was successfully applied to real water samples as a SPE sorbent.

Acknowledgments

This work has been completed with the financial support of the University of Malaya Research Grant (RP 006A-13SUS), IPPP grant (PV 076/2012A) and High Impact Research (HIR) Grant under Ministry of Higher Education (HIR/MOHE/SC/F00031). The authors gratefully acknowledge the Department of Chemistry, University of Malaya and Ministry of Higher Education Malaysia for their financial support through MyPhD scholarship to the researcher named Hemavathy Surikumaran.

Supplementary data

Supplemental data for this article can be accessed here http://10.1080/19443994.2015.1012333.

Symbols

K_d — distribution coefficient
C_i — initial concentration of 2,4-dichlorophenol solution
C_f — final concentration of 2,4-dichlorophenol solution
v — volume of 2,4-dichlorophenol solution used
M — weight of MIP MAA-βCD used
k — selectivity coefficient
k' — relative selectivity coefficient

References

[1] T. Saitoh, K. Asano, M. Hiraide, Polyallylamine-conjugated thermo-responsive polymers for the rapid removal of phenolic compounds from water, React. Funct. Polym. 72 (2012) 317–322.
[2] B. Antizar-Ladislao, N.I. Galil, Biosorption of phenol and chlorophenols by acclimated residential biomass under bioremediation conditions in a sandy aquifer, Water Res. 38 (2004) 267–276.
[3] M. Radhika, K. Palanivelu, Adsorptive removal of chlorophenols from aqueous solution by low cost adsorbent—Kinetics and isotherm analysis, J. Hazard. Mater. 138 (2006) 116–124.
[4] L. Keith, W. Telliard, ES&T special report: Priority pollutants: I-a perspective view, Environ. Sci. Technol. 13 (1979) 416–423.
[5] B. Bukowska, Effects of 2,4-D and its metabolite 2,4-dichlorophenol on antioxidant enzymes and level of glutathione in human erythrocytes, Comp. Biochem. Physiol. C: Toxicol. Pharmacol. 135 (2003) 435–441.
[6] M.A. Ashraf, M. Hussain, K. Mahmood, A. Wajid, M. Yusof, Y. Alias, I. Yusoff, Removal of acid yellow-17 dye from aqueous solution using eco-friendly biosorbent, Desalin. Water Treat. 51 (2013) 4530–4545.
[7] N.H. Hussin, I. Yusoff, Y. Alias, S. Mohamad, N.Y. Rahim, M.A. Ashraf, Ionic liquid as a medium to remove iron and other metal ions: A case study of the North Kelantan aquifer, Malaysia, Environ. Earth Sci. 71 (2014) 2105–2113.
[8] N. Calace, E. Nardi, B.M. Petronio, M. Pietroletti, Adsorption of phenols by papermill sludges, Environ. Pollut. 118 (2002) 315–319.
[9] A. Bhatnagar, A. Minocha, Adsorptive removal of 2, 4-dichlorophenol from water utilizing *Punica granatum* peel waste and stabilization with cement, J. Hazard. Mater. 168 (2009) 1111–1117.
[10] G. Rojas, J. Silva, J.A. Flores, A. Rodriguez, M. Ly, H. Maldonado, Adsorption of chromium onto cross-linked chitosan, Sep. Purif. Technol. 44 (2005) 31–36.
[11] Y.P. Chin, S. Mohamad, M.R.B. Abas, Removal of parabens from aqueous solution using β-cyclodextrin cross-linked polymer, Int. J. Mol. Sci. 11 (2010) 3459–3471.
[12] J. Pan, X. Zou, X. Wang, W. Guan, Y. Yan, J. Han, Selective recognition of 2,4-dichlorophenol from aqueous solution by uniformly sized molecularly imprinted microspheres with β-cyclodextrin/attapulgite composites as support, Chem. Eng. J. 162 (2010) 910–918.
[13] Y. Li, X. Li, C. Dong, Y. Li, P. Jin, J. Qi, Selective recognition and removal of chlorophenols from aqueous solution using molecularly imprinted polymer prepared by reversible addition-fragmentation chain transfer polymerization, Biosens. Bioelectron. 25 (2009) 306–312.
[14] Y. Li, X. Li, Y. Li, J. Qi, J. Bian, Y. Yuan, Selective removal of 2,4-dichlorophenol from contaminated water using non-covalent imprinted microspheres, Environ. Pollut. 157 (2009) 1879–1885.
[15] M. Komiyama, T. Takeuchi, T. Mukawa, H. Asanuma, Molecular Imprinting: From Fundamentals to Applications, vol. 1, Wiley-VCH, 2003, p. 148, ISBN 3-527-30569-6.
[16] S. Piletsky, A.P. Turner, Molecular imprinting of polymers, Landes Biosciences, Georgetown, TX, 2006.
[17] M. Gallego-Gallegos, R. Muñoz-Olivas, C. Cámara, Different formats of imprinted polymers for determining organotin compounds in environmental samples, J. Environ. Manage. 90 (2009) S69–S76.
[18] B. Sellergren, Imprinted chiral stationary phases in high-performance liquid chromatography, J. Chromatogr. A 906 (2001) 227–252.
[19] V. Pichon, F. Chapuis-Hugon, Role of molecularly imprinted polymers for selective determination of environmental pollutants—A review, Anal. Chim. Acta 622 (2008) 48–61.
[20] F. Chapuis, J.U. Mullot, V. Pichon, G. Tuffal, M.C. Hennion, Molecularly imprinted polymers for the clean-up of a basic drug from environmental and biological samples, J. Chromatogr. A 1135 (2006) 127–134.
[21] V. Pichon, Selective sample treatment using molecularly imprinted polymers, J. Chromatogr. A 1152 (2007) 41–53.
[22] J. Li, J. Zhao, X. Wei, A sensitive and selective sensor for dopamine determination based on a molecularly imprinted electropolymer of o-aminophenol, Sens. Actuators B 140 (2009) 663–669.
[23] C. Alexander, L. Davidson, W. Hayes, Imprinted polymers: Artificial molecular recognition materials with applications in synthesis and catalysis, Tetrahedron 59 (2003) 2025–2057.
[24] W.B. Motherwell, M.J. Bingham, Y. Six, Recent progress in the design and synthesis of artificial enzymes, Tetrahedron 57 (2001) 4663–4686.

[25] O. Ramström, K. Mosbach, Synthesis and catalysis by molecularly imprinted materials, Curr. Opin. Chem. Biol. 3 (1999) 759–764.
[26] X. Xu, L. Zhu, L. Chen, Separation and screening of compounds of biological origin using molecularly imprinted polymers, J. Chromatogr. B 804 (2004) 61–69.
[27] D.L. Rathbone, Molecularly imprinted polymers in the drug discovery process, Adv. Drug Deliv. Rev. 57 (2005) 1854–1874.
[28] O. Ramström, L. Ye, K. Mosbach, Screening of a combinatorial steroid library using molecularly imprinted polymers, Anal. Commun. 35 (1998) 9–11.
[29] J. Berglund, C. Lindbladh, K. Mosbach, I.A. Nicholls, Selection of phage display combinatorial library peptides with affinity for a yohimbine imprinted methacrylate polymer, Anal. Commun. 35 (1998) 3–7.
[30] C. Alvarez-Lorenzo, A. Concheiro, Molecularly imprinted polymers for drug delivery, J. Chromatogr. B 804 (2004) 231–245.
[31] D. Cunliffe, A. Kirby, C. Alexander, Molecularly imprinted drug delivery systems, Adv. Drug Delivery Rev. 57 (2005) 1836–1853.
[32] A.G. Mayes, M.J. Whitcombe, Synthetic strategies for the generation of molecularly imprinted organic polymers, Adv. Drug Delivery Rev. 57 (2005) 1742–1778.
[33] L.q. Guo, Y.b. Zeng, A.h. Guan, G.n. Chen, Preparation and characterization of molecularly imprinted silica particles for selective adsorption of naphthalene, React. Funct. Polym. 71 (2011) 1172–1176.
[34] S.A. Piletsky, S. Alcock, A.P. Turner, Molecular imprinting: At the edge of the third millennium, Trends Biotechnol. 19 (2001) 9–12.
[35] X. Huang, L. Kong, X. Li, C. Zheng, H. Zou, Molecular imprinting of nitrophenol and hydroxybenzoic acid isomers: Effect of molecular structure and acidity on imprinting, J. Mol. Recognit. 16 (2003) 406–411.
[36] P. Luliński, D. Maciejewska, Impact of functional monomers, cross-linkers and porogens on morphology and recognition properties of 2-(3,4-dimethoxyphenyl) ethylamine imprinted polymers, Mater. Sci. Eng. C 31 (2011) 281–289.
[37] G.Z. Kyzas, N.K. Lazaridis, D.N. Bikiaris, Optimization of chitosan and β-cyclodextrin molecularly imprinted polymer synthesis for dye adsorption, Carbohydr. Polym. 91 (2013) 198–208.
[38] J. Szejtli, Introduction and general overview of cyclodextrin Chemistry, Chem. Rev. 98 (1998) 1743–1754.
[39] G. Crini, G. Torri, Y. Lekchiri, B. Martel, L. Janus, M. Morcellet, High performance liquid chromatography of structural isomers using a cyclodextrin-poly(allylamine) coated silica column, Chromatographia 41 (1995) 424–430.
[40] A. Romo, F.J. Peñas, J.R. Isasi, I.X. García-Zubiri, G. González-Gaitano, Extraction of phenols from aqueous solutions by β-cyclodextrin polymers. Comparison of sorptive capacities with other sorbents, React. Funct. Polym. 68 (2008) 406–413.
[41] L. Janus, G. Crini, V. El-Rezzi, M. Morcellet, A. Cambiaghi, G. Torri, A. Naggi, C. Vecchi, New sorbents containing beta-cyclodextrin. Synthesis, characterization, and sorption properties, React. Funct. Polym. 42 (1999) 173–180.
[42] Z. Xu, L. Xu, D. Kuang, F. Zhang, J. Wang, Exploiting β-cyclodextrin as functional monomer in molecular imprinting for achieving recognition in aqueous media, Mater. Sci. Eng. C 28 (2008) 1516–1521.
[43] I. Suzuki, Y. Egawa, Y. Mizukawa, T. Hoshi, J.-I. Anzai, Construction of positively-charged layered assemblies assisted by cyclodextrin complexation, Chem. Commun. 2 (2002) 164–165.
[44] K. Yongfeng, D. Wuping, L. Yan, K. Junxia, X. Jing, Molecularly imprinted polymers of allyl-β-cyclodextrin and methacrylic acid for the solid-phase extraction of phthalate, Carbohydr. Polym. 88 (2012) 459–464.
[45] N. Pariot, F. Edwards-Lévy, M.C. Andry, M.C. Lévy, Cross-linked β-cyclodextrin microcapsules. II. Retarding effect on drug release through semi-permeable membranes, Int. J. Pharm. 232 (2002) 175–181.
[46] N. Holland, J. Frisby, E. Owens, H. Hughes, P. Duggan, P. McLoughlin, The influence of polymer morphology on the performance of molecularly imprinted polymers, Polymer 51 (2010) 1578–1584.
[47] K. Sreenivasan, Synthesis and evaluation of a beta cyclodextrin-based molecularly imprinted copolymer, J. Applied Polym. Sci. 70 (1998) 15–18.
[48] E. Caro, R.M. Marcé, P.A.G. Cormack, D.C. Sherrington, F. Borrull, On-line solid-phase extraction with molecularly imprinted polymers to selectively extract substituted 4-chlorophenols and 4-nitrophenol from water, J. Chromatogr. A 995 (2003) 233–238.
[49] B. Cwiertnia, T. Hladon, M. Stobiecki, Stability of diclofenac sodium in the inclusion complex with β-cyclodextrin in the solid state, J. Pharm. Pharmacol. 51 (1999) 1213–1218.
[50] G. Oertel, Polyurethane Handbook: Chemistry, Raw Materials, Processing, Application, Properties. Hanser, Munich, 1985.
[51] H. Asanuma, M. Kakazu, M. Shibata, T. Hishiya, Molecularly imprinted polymer of β-cyclodextrin for the efficient recognition of cholesterol, Chem. Commun. (1997) 1971–1972.
[52] İ. Abay, A. Denizli, E. Bişkin, B. Salih, Removal and pre-concentration of phenolic species onto β-cyclodextrin modified poly(hydroxyethylmethacrylate–ethyleneglycoldimethacrylate) microbeads, Chemosphere 61 (2005) 1263–1272.
[53] G.P. González, P.F. Hernando, J. Alegría, A morphological study of molecularly imprinted polymers using the scanning electron microscope, Anal. Chim. Acta 557 (2006) 179–183.
[54] L. Wang, J. Zhang, R. Zhao, C. Zhang, C. Li, Y. Li, Adsorption of 2,4-dichlorophenol on Mn-modified activated carbon prepared from *Polygonum orientale* Linn. Desalination 266 (2011) 175–181.
[55] S. Mohamad, H. Surikumaran, M. Raoov, T. Marimuthu, K. Chandrasekaram, P. Subramaniam, Conventional study on novel dicationic ionic liquid inclusion with β-cyclodextrin, Int. J. Mol. Sci. 12 (2011) 6329–6345.
[56] K.L. Salipira, R.W. Krause, B.B. Mamba, T.J. Malefetse, L.M. Cele, S.H. Durbach, Cyclodextrin polyurethanes polymerized with multi-walled carbon nanotubes: Synthesis and characterization, Mater. Chem. Phys. 111 (2008) 218–224.

[57] P. Qi, J. Wang, J. Jin, F. Su, J. Chen, 2,4-Dimethylphenol imprinted polymers as a solid-phase extraction sorbent for class-selective extraction of phenolic compounds from environmental water, Talanta 81 (2010) 1630–1635.
[58] H. Yan, K.H. Row, Characteristic and synthetic approach of molecularly imprinted polymer, Int. J. Mol. Sci. 7 (2006) 155–178.
[59] J. Fan, Y. Wei, J. Wang, C. Wu, H. Shi, Study of molecularly imprinted solid-phase extraction of diphenylguanidine and its structural analogs, Anal. Chim. Acta 639 (2009) 42–50.
[60] W. Zhang, L. Qin, R.-R. Chen, X.-W. He, W.-Y. Li, Y.-K. Zhang, Protein imprinted polymer using acryloyl-β-cyclodextrin and acrylamide as monomers, Appl. Surf. Sci. 256 (2010) 3000–3005.
[61] K. Hanna, C. de Brauer, P. Germain, Solubilization of the neutral and charged forms of 2,4,6-trichlorophenol by β-cyclodextrin, methyl-β-cyclodextrin and hydroxypropyl-β-cyclodextrin in water, J. Hazard. Mater. 100 (2003) 109–116.
[62] E. Leyva, E. Moctezuma, J. Strouse, M.A. García-Garibay, Spectrometric and 2D NMR studies on the complexation of chlorophenols with cyclodextrins, J. Inclusion Phenom. Macrocyclic Chem. 39 (2001) 41–46.
[63] J. Li, X. Ni, Z. Zhou, K.W. Leong, Preparation and characterization of polypseudorotaxanes based on block-selected inclusion complexation between poly (propylene oxide)-poly(ethylene oxide)-poly(propylene oxide) triblock copolymers and α -cyclodextrin, J. Am. Chem. Soc. 125 (2003) 1788–1795.
[64] A. Ersöz, A. Denizli, İ. Şener, A. Atılır, S. Diltemiz, R. Say, Removal of phenolic compounds with nitrophenol-imprinted polymer based on π–π and hydrogen-bonding interactions, Sep. Purif. Technol. 38 (2004) 173–179.